PROCEEDINGS OF SCIENCE

An Overview of Helions in the HSR and its Injectors

Kiel Hock,[a,*] **Haixin Huang,**[a] **François Méot,**[a] **Vadim Ptitsyn,**[a] **Vahid Ranjbar**[a] **and Vincent Schoefer**[a]

[a] *Brookhaven National Laboratory Collider-Accelerator Department, Upton, NY United States*

E-mail: khock@bnl.gov

The Electron Ion Collider (EIC) calls for polarized helion on polarized electron collisions. These collisions will require 1.2×10^{11} ions per bunch at 70% polarization. Meeting the EIC physics requirements will require maintaining both high efficiency and high polarization transmission through the accelerator complex. Polarized helions will originate from the Electron Beam Ion Source (EBIS) and be injected into the Booster at $|G\gamma| = 4.1932$. The injected intensity from EBIS is expected to be 2×10^{11} ions with a polarization of 80%. In the Booster, an AC dipole will be used to spin-flip across intrinsic resonances and harmonic corrections will be used for imperfection resonances, up to extraction at $|G\gamma|$=10.5. In the Alternating Gradient Synchrotron (AGS), due to the higher anomalous g-factor of helions, the two partial snakes will have sufficient rotation to facilitate both horizontal and vertical betatron tunes being placed inside the spin-tune gap up to $|G\gamma|$=49.5. In the Hadron Storage Ring (HSR), 6 full snakes will be used to minimize polarization loss up to a maximum energy of $|G\gamma|$=820. At collisions, longitudinal polarization will be available through use of helical spin rotators. This paper provides a summary of polarized helion transmission from injection to the Booster to top energy in the Hadron Storage Ring.

25th International Spin Physics Symposium
Durham Convention Center
September 24-29

*Speaker

PoS(SPIN2023)095

1. Introduction

Polarized neutron collisions are part of the Electron Ion Collider (EIC) physics program, which will be facilitated with collisions of polarized helions, where up to 86% of the polarization is accounted for by the neutron [1][2][3]. The Relativistic Heavy Ion Collider (RHIC) is scheduled to run until 2025, followed by EIC construction from 2025 through 2032. The layout of the EIC is seen in Fig. 1 [4]. The construction involves the installation of the electron accelerator and collider rings inside the existing RHIC tunnel while also reconfiguring the existing RHIC into the Hadron Storage Ring (HSR). The EIC commissioning and physics program will follow. The existing injector chain for RHIC will be reused, which consists of the Alternating Gradient Synchrotron (AGS), the AGS Booster (or Booster), and the AGS to RHIC transfer line (ATR).

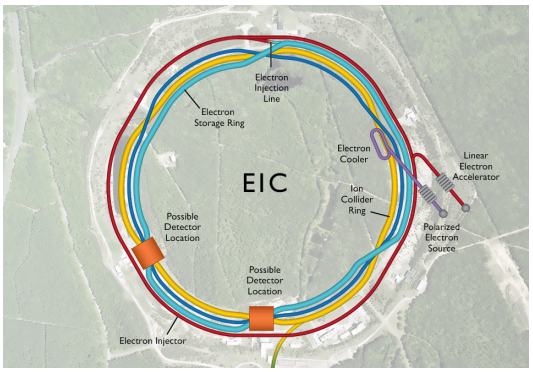

Figure 1: Layout of the Electron Ion Collider.

The equation of motion for a particle's spin with given vector, $\vec{S}$, in a synchrotron is given by the Thomas-BMT equation (neglecting effects of $\vec{E}$) [5]

$$\frac{d\vec{S}}{dt} = \frac{q}{\gamma m}\vec{S} \times \left[(1+G\gamma)\vec{B}_{\perp} + (1+G)\vec{B}_{\parallel}\right] \tag{1}$$

where γ is the Lorentz factor, m is the mass, q is the charge, G is the anomalous gyromagnetic g-factor, and $\vec{B}_{\perp}$ and $\vec{B}_{\parallel}$ are the transverse and longitudinal magnetic fields. Here, $\vec{B}_{\perp}$ is strongest due to presence of strong focusing quadrupoles and $\vec{B}_{\parallel}$ is small. From this, the vertical resonance strengths can be calculated with the Fourier transform of spin perturbing fields [6]

$$\epsilon_k = \frac{(1+G\gamma)}{2\pi} \oint \left[\frac{\partial B_x/\partial y}{B\rho}\right] y e^{iK\theta} ds \tag{2}$$

where $\partial B_x/\partial y$ is the field gradient, $B\rho$ is the reference rigidity, θ is the location in the ring, and K is the resonance condition. This equation is satisfied when $K = \nu_s = n$ and $K = \nu_s = nP \pm \nu_y$, where n is an integer, P is the superperiodicity, and ν_y is the vertical betatron tune. The anomalous gyromagnetic g-factor for helions, G=-4.184154=G_h, is several times larger than that of protons, G_p=1.792847. The energy spacing between imperfection resonances is [7],

$$\Delta_{imp} = \frac{m}{qG}. \tag{3}$$

The spacing between these resonances for protons is Δ_{imp}=523.34 MeV whereas the spacing for helions is Δ_{imp}=335.60 MeV. By comparing the two spacings, one can infer that helions will cross 1.56 more resonances per unit change in energy.

2. Polarized Helions in the AGS Booster

Polarized helions are provided by Electron Beam Ion Source (EBIS) and the injected intensity into the Booster is expected to be $2{\times}10^{11}$ with a polarization of 80%. Polarized helions are injected into the Booster at $|G\gamma| = 4.19$. At injection, $\nu_y < 4.1$ to avoid the $|G\gamma| = 0 + \nu_y$ resonance. Extraction is possible at $|G\gamma| = 7.5$ and $|G\gamma| = 10.5$, as seen in Fig. 2, to match the stable spin direction between Booster and AGS.

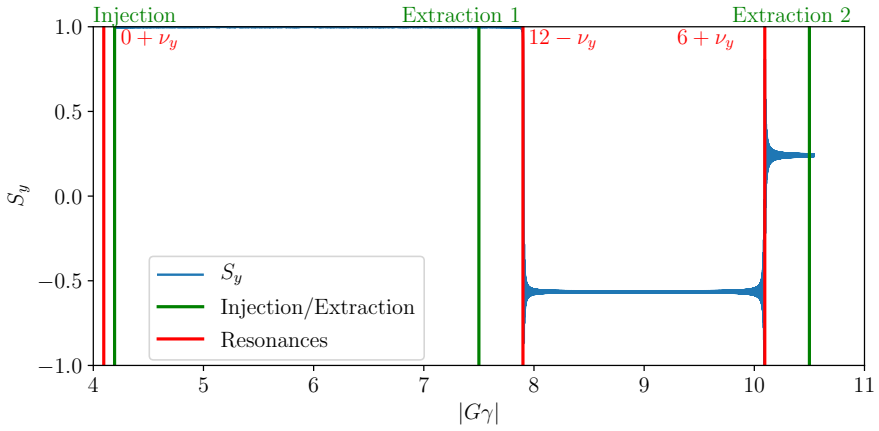

Figure 2: Image of the Booster cycle with the two extraction points, and three possible intrinsic resonances.

In the case of extraction from the Booster at $|G\gamma| = 10.5$, helions will cross the $|G\gamma| = 5$ through 10 imperfection resonances, and the $|G\gamma| = 12 - \nu_y$ and $|G\gamma| = 6 + \nu_y$ vertical intrinsic resonances. This higher extraction energy allows for stronger snakes in the AGS which will allow the vertical tune to be placed inside spin tune gap in AGS at injection, which is discussed in detail in Sec. 3 [8]. This higher energy also minimizes optical defects from AGS cold snake as seen in Fig. 4 [9].
In the case of extraction at $|G\gamma| = 7.5$, helions will cross the $|G\gamma| = 5$ through 7 imperfection resonance, and all intrinsic resonances can be avoided. The caveat of this lower injection energy is insufficient dynamic aperture to allow both the horizontal and vertical tunes inside the spin tune gap at injection. This will lead to polarization and beam loss.

2.1 Intrinsic Resonance Crossing

To facilitate lossless polarization transmission through the intrinsic resonances in the Booster up to $|G\gamma| = 10.5$, an AC dipole has been installed [10]. An AC dipole drives large amplitude vertical betatron oscillations of all particles with a horizontal magnetic field that oscillates in phase with the vertical betatron motion. The AC dipole tune is $\nu_m = f_m/f_{rev}$ with f_m is the AC dipole frequency [11]. The amplitude of these coherent oscillations is

$$Y_{coh} = \frac{B_m l}{4\pi B\rho \delta_m}\beta_y \tag{4}$$

where $B_m l$ is the integrated strength of the dipole kick, δ_m is the resonance proximity parameter, and β_y is the vertical beta function. The resonance proximity parameter is the separation between ν_m and ν_y, that is $\delta_m = \nu_y - (n + \nu_m)$. This creates a driven resonance at ν_m.

Here f_m is fixed as it is matched using capacitors to the resonant circuit. As a result, ν_m can change as much as $\Delta\nu_m = 0.0028$ for helions crossing $|G\gamma| = 12 - \nu_y$ due to the rapid change in f_{rev}. This is solved by putting a slope on the tune settings for the range of the AC dipole pulse. A full spin-flip is achieved with $B_m l = 16.5$ G · m ($|G\gamma| = 12 - \nu_y$) and $B_m l = 20.5$ G · m ($|G\gamma| = 6 + \nu_y$), as seen in Fig. 3. The AC dipole has been designed with a maximum strength of $B_m l = 25$ G · m [12].

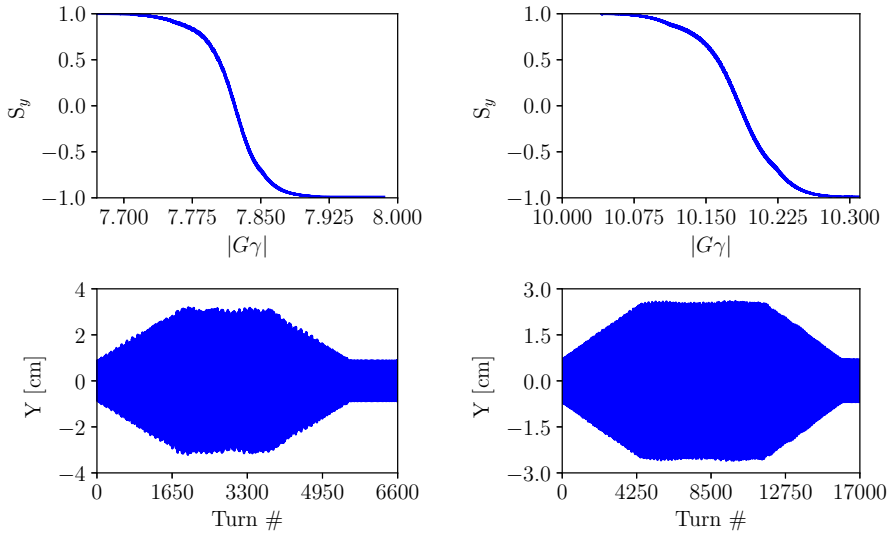

Figure 3: AC dipole simulations using zgoubi for the $|G\gamma| = 12 - \nu_y$ (left) and $|G\gamma| = 6 + \nu_y$ (right) intrinsic resonances.

2.2 Imperfection Resonance Crossings

To facilitate lossless polarization transmission through imperfection resonances in the Booster, the harmonic correction method will be used. For correcting the $|G\gamma| = k$ resonance, the $h = k$ harmonic of the corrector dipoles is used. At each resonance, the harmonic h=k can either be: corrected so no polarization is lost, or enhanced to induce a full spin-flip. [13]
The Booster has 24 vertical orbit correctors placed adjacent to vertically focusing quadrupoles, and are used for creating and correcting orbit harmonics. These correctors are powered according to

$$B_{j,h} = a_h \sin(h\theta_j) + b_h \cos(h\theta_j) \tag{5}$$

where j is corrector number, θ_j is the location in the ring, a_h and b_h are the amplitudes for harmonic h.
The total current on corrector j is

$$I_j = \sum_h I_{h,S} \sin(h\theta_j) + I_{h,C} \cos(h\theta_j) \tag{6}$$

where $I_{h,S}$ and $I_{h,C}$ are the corrector currents for the Sine and Cosine components. The maximum current of all correctors is

$$I_{max} = \max[|I_j|]. \tag{7}$$

This is an important parameter so as to avoid exceeding the maximum current of the supplies, 25 A. The Froissart-Stora formula at a given resonance k, and harmonic h=k, as a function of corrector current is given by [6],

$$\frac{P_f}{P_i} = 2e^{-\frac{(I_{k,S}-\mu_{k,S})^2}{2\sigma_{k,S}^2}} e^{-\frac{(I_{k,C}-\mu_{k,C})^2}{2\sigma_{k,C}^2}} - 1 \tag{8}$$

where P_f is the final asymptotic polarization after crossing the resonance, P_i is the initial asymptotic polarization before crossing the resonance, $\mu_{k,S}$ and $\mu_{k,C}$ are the optimal corrector currents to correct the h=k harmonic, and $\sigma_{k,S}$ and $\sigma_{k,C}$ are the widths of the distributions. A summary of minimum current required to excite the harmonic and induce a spin-flip, $I_{M,F}$, and the current to correct the harmonic for zero polarization loss, $I_{M,C}$ is summarized in Tab. 1.

Table 1: Table summarizing corrector current requirements for each imperfection resonance crossing, including the current for h=5 correction.

K	μ_S [A]	μ_C [A]	$I_{S,K}$	$I_{C,K}$	$I_{M,F}$	$I_{M,C}$
5	0.322	2.105	0.35	-1.71	4.33	6.44
6	0.567	-0.189	1.78	9.65	17.77	9.19
7	1.425	0.847	10.02	-8.14	22.4	13.95
8	-2.463	5.242	2.75	-9.39	21.98	22.37
9	-0.614	-0.222	-1.17	-14.35	29.71	17.59
10	-23.669	-0.477	-3.67	-0.477	22.86	39.43

3. Polarized Helions in the AGS

3.1 AGS Admittance at Injection

To quantify the optical defects, particles are tracked through only the cold snake to calculate the transport matrix. From the transport matrix, the total coupling (CP) and focusing (FC) are calculated from transport matrix elements m_{ij} [9],

$$CP = LL + UR \tag{9}$$

with

$$LL = m_{31}^2 + m_{32}^2 + m_{41}^2 + m_{42}^2 \tag{10}$$

$$UR = m_{13}^2 + m_{14}^2 + m_{23}^2 + m_{24}^2. \tag{11}$$

and

$$FC = m_{12}^2 + m_{34}^2 \tag{12}$$

These optical distortions reduce exponentially with $B\rho$ as seen in Fig. 4. Increases in $B\rho$ show a substantial increase in admittance, as seen in Fig. 5.

An example of the horizontal and vertical tunes, along with spin tune and the projection of the stable spin direction on the vertical axis is shown in Fig. 6. At $G\gamma$=8, the $G\gamma = 8 \pm \nu_x$ and $G\gamma = 8 \pm \nu_y$ are potentially crossed. The optimal transmission of helions up to $|G\gamma| = 10.5$ in the

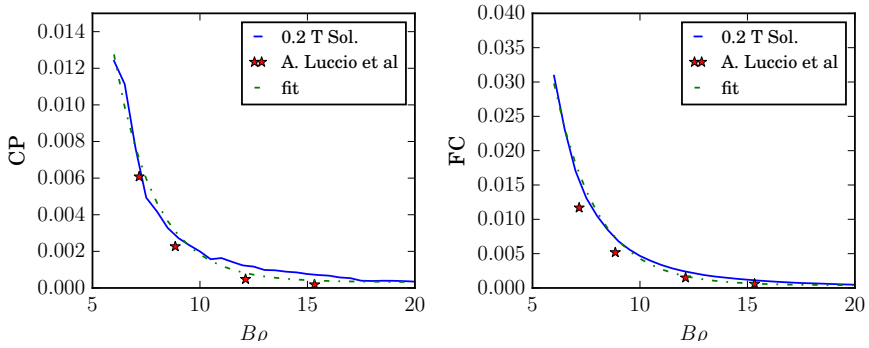

Figure 4: Coupling and focusing from the AGS cold snake as a function of $B\rho$ and comparison to an exponential fit.

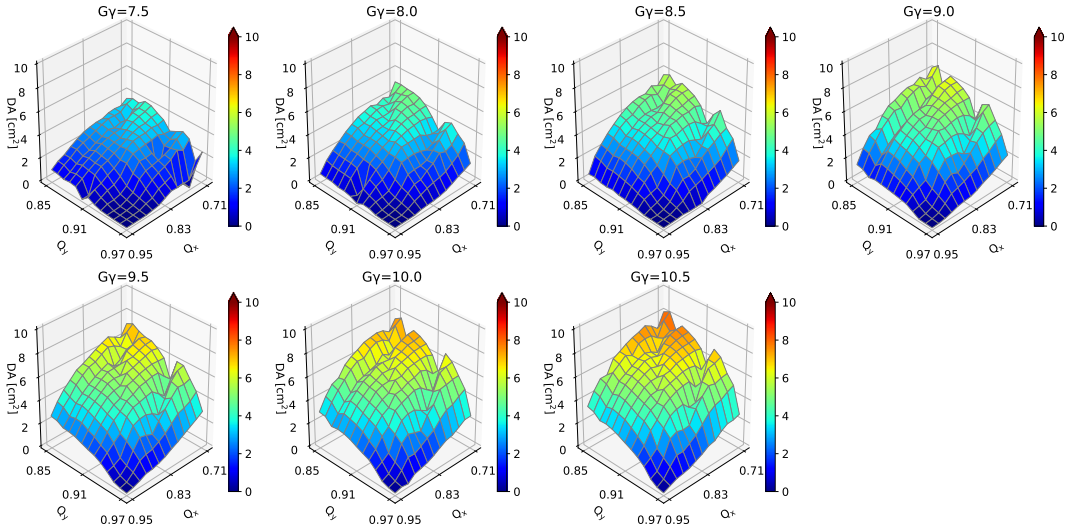

Figure 5: Dynamic aperture in the region of interest from $|G\gamma| = 7.5$ to $|G\gamma| = 10.5$ with spacing of 0.5 units of $|G\gamma|$.

AGS if extraction occurs at $|G\gamma| = 7.5$, is summarized in Table 2. Due to the reduced admittance at $|G\gamma| = 7.5$, the excessive beam loss will necessitate additional bunch merges compared to the $|G\gamma| = 10.5$ case.

Table 2: Polarization and beam loss considered at integer values of $|G\gamma|$ from $|G\gamma| = 7.5$ to $|G\gamma| = 10.5$ to quantify beam and polarization losses in the case that helions are injected at $|G\gamma| = 7.5$.

$\lvert G\gamma\rvert$	ν_x	ν_y	Beam loss	Polarization
7.5 to 8.5	8.88	8.94	76.7%	98.7%
8.5 to 9.5	8.82	8.94	0.2%	99.0%
9.5 to 10.5	8.92	8.96	14.7%	99.7%

To support $|G\gamma| = 10.5$ injection, the Booster Main Magnet power supply and AGS injection kicker need to be upgraded.

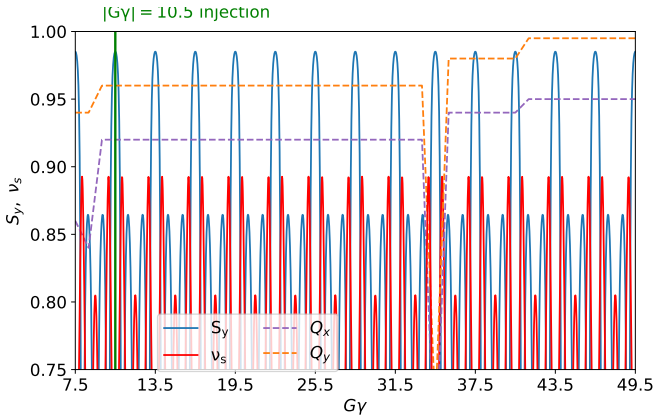

Figure 6: Spin tune, the projection of the stable spin direction on the vertical axis, and the horizontal and vertical tune paths as a function of $|G\gamma|$.

Crossing of the strong $|G\gamma| = 36 + \nu_y$ resonance with tracking up to extraction at $|G\gamma| = 49.5$ is shown in Fig. 7 and exhibits no loss of polarization.

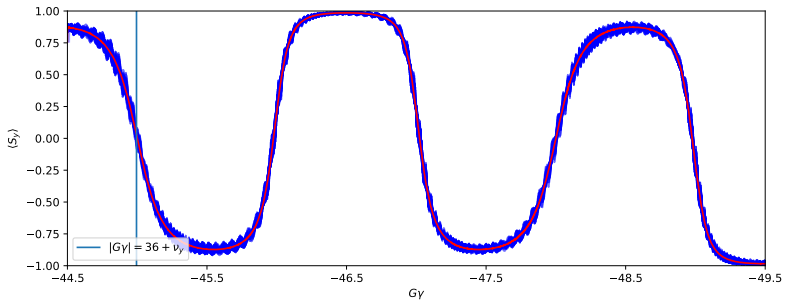

Figure 7: A bunch of 1,000 particles tracked from $|G\gamma| = 45.5$ to extraction at $|G\gamma| = 49.5$ without any polarization loss.

3.2 Extraction from AGS

Extraction from the AGS to the HSR occurs at $|G\gamma| = 49.5$, and avoids crossing the strong $|G\gamma| = 60 - \nu_y \sim 51$. Due to the mismatch in stable spin direction between the end of ATR and at the AGS extraction septum, extraction cannot occur above $|G\gamma| = 51.5$ [14]. This is lower in rigidity ($B\rho = 55.21$ Tm) than protons which extract at $G\gamma = 45.5$ ($B\rho = 79.37$ Tm).

4. Polarized Helions in the HSR

4.1 HSR Resonance Strengths

The resonance spectra is calculated from Eq. 2 and is evaluated from injection at $|G\gamma| = 49.5$ to the maximum energy corresponding to $|G\gamma| = 820$. The resonance strength for the $|G\gamma| = 400$ region is comparable to the $|G\gamma| = 700$ region. The $|G\gamma| = 412 - \nu_y$ resonance is strong but well isolated. This is unlike the $|G\gamma| = 718 + \nu_y$ resonance where several strong nearby resonances

located at $|G\gamma| = 715 + \nu_y$, $716 + \nu_y$, and $717 + \nu_y$. Each of these resonances are stronger than the strongest proton resonance. The resonance structure in proximity of the $|G\gamma| = 734 - \nu_y$ region is similar, albeit with slightly more spacing. Polarization transmission studies are ongoing.

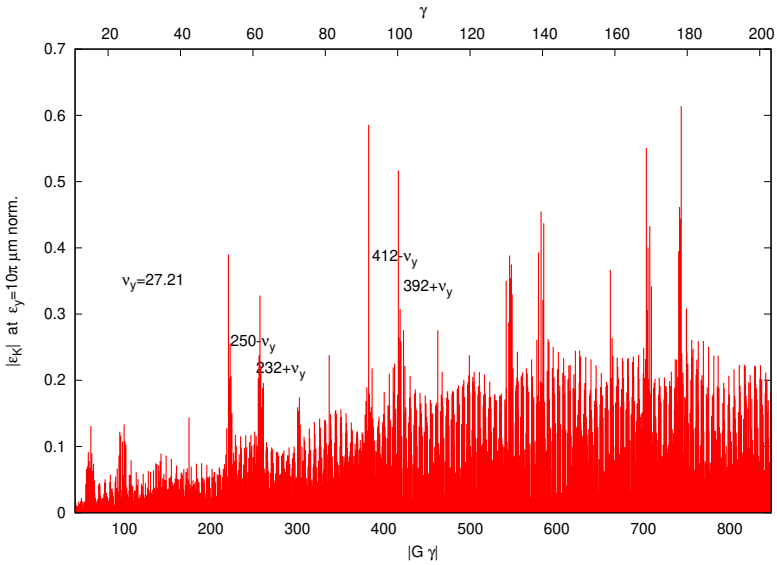

Figure 8: HSR resonance spectra of helions.

4.2 HSR Rotators

The existing RHIC rotators will be reused for the HSR [15]. Each rotator consist of four helical dipoles in series where the two outer coils are powered separately from the two inner coils [16]. The HSR rotators are located at θ=61.35 mrad and θ=-17 mrad away from IP6, where RHIC rotators are at θ =3.675 and -3.675 mrad, with θ being the bending angle [15]. For the angle to be longitudinal at IP6, the angle at each rotator in the horizontal plane is

$$\phi = G\gamma\theta \tag{13}$$

The power supply limit for the inner and outer coils is 322 A, which corresponds to a field of 4 T [17].
Due to the higher G of helions, the current requirements are well below the ±322 A as seen in Fig. 9. The three desired energies for collisions: 41 GeV, 100 GeV, and 820 GeV are marked and the power supply requirements at those energies are giving in Table 3.

Table 3: Table of power supply currents for the sector 5 (Rot5) and sector 6 (Rot6) at 41, 100, and 183 GeV.

Energy (GeV)	Rot5		Rot6	
	Outer	Inner	Outer	Inner
41	152.6	119.3	167.8	144.5
100	47.1	178.5	68.4	153.9
183	160.7	126.1	65.4	156.0

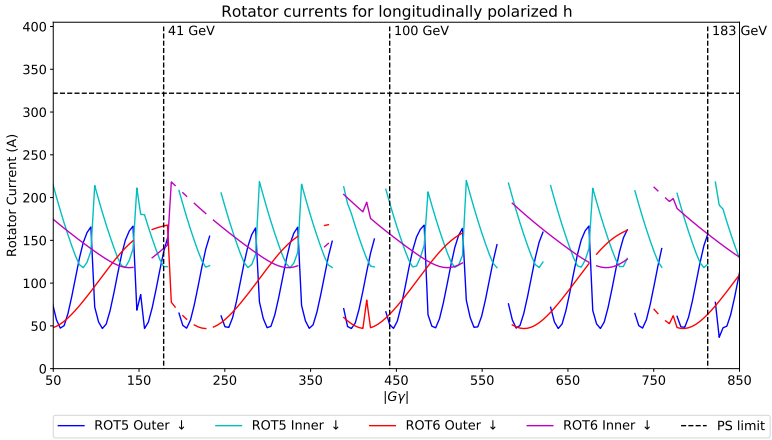

Figure 9: Rotator currents for the inner and outer power supplies for the sector 5 and sector 6 rotators.

5. Summary

The AC dipole is able to spin-flip through the two intrinsic resonances in Booster. The harmonic correction method allows for 100% polarization transmission through the six imperfection resonances. The higher injection $|G\gamma|$ into AGS allows for stronger snake settings. These stronger snakes allow both horizontal and vertical tunes to be placed inside the spin tune gap. This precludes the need of tune jumps and emittance growth associated with it. Extraction from the AGS at $|G\gamma| = 49.5$ provides the best spin match from AGS to the HSR and avoids the $|G\gamma| = 60 - \nu_y$ resonance. An intensity of $1.5{\times}10^{11}$ ions/bunch with a polarization of 75-78% is expected at extraction. Current RHIC rotators and their power supplies can be reused in the HSR and will operate below the power supply limits. HSR resonance crossing simulations are ongoing.

6. Acknowledgements

The work is supported by Brookhaven Science Associates, LLC under Contract No. DE-SC0012704 with the U.S. Department of Energy.

References

[1] E. Aschenauer et al. Opportunities for Polarized He-3 in RHIC and EIC. In *Proceedings of RIKEN BNL Research Center Workshop*, 2011. URL https://www.bnl.gov/isd/documents/76833.pdf.

[2] W. Fischer et al. eRHIC in electron-ion operation. In *10th International Particle Accelerator Conference (IPAC19) Conference. Melbourne, Australia*, 2019. URL https://www.osti.gov/servlets/purl/1515151.

[3] G. Zschornacka et al. Electron beam ion sources, 2014. URL https://arxiv.org/pdf/1410.8014.pdf.

[4] F. Willeke et al. Electron ion collider conceptual design report 2021. doi: 10.2172/1765663. URL https://www.osti.gov/biblio/1765663.

[5] L. Michel V. Bargmann and V. L. Telegdi. Precession of the polarization of particles moving in a homogeneous electromagnetic field. *Phys. Rev. Lett.*, 2:435–436, May 1959. doi: 10.1103/PhysRevLett.2.435. URL https://link.aps.org/doi/10.1103/PhysRevLett.2.435.

[6] S. Y. Lee. *Spin Dynamics and Snakes in Synchrotrons*. World Scientific Publishing Company Incorporated, 1997.

[7] K. Hock. *Transport of Polarized helions in Injector Synchrotrons for the future electrion0ion collider project at the Brookhaven National Laboratory*. PhD thesis, University Grenoble-Alpes, October 2021. URL https://www.theses.fr/2021GRALY056.pdf.

[8] K. Hock et al. AGS Dynamic Aperture at Injection of Polarized Protons and helions. In *Proc. 11th International Partile Accelerator Conference (IPAC'21), Campinas, Brazil, 24-28 May 2021*, May 2021.

[9] A. Luccio et al. *Cold AGS Snake Optimization by Modeling*. C-AD Tech Note 128, 2003. URL https://technotes.bnl.gov/PDF?publicationId=32092.

[10] K. Hock et al. Commissioning results of the bnl alternating gradient synchrotron booster ac dipole. *Nuclear Instruments and Methods in Physics Research Section A: Accelerators, Spectrometers, Detectors and Associated Equipment*, 1059:168999, 2024. ISSN 0168-9002. doi: https://doi.org/10.1016/j.nima.2023.168999. URL https://www.sciencedirect.com/science/article/pii/S0168900223009993.

[11] M. Bai. *Overcoming the Intrinsic Spin Resonance by Using an RF Dipole*. PhD thesis, Indiana University, 1999. URL https://www.rhichome.bnl.gov/RHIC/Spin/papers/baithesis.pdf.

[12] N. Tsoupas et al. An AC Dipole for the AGS Booster to overcome spin resonances. In *Proceedings CAARI 2018 Conference*. Dallas, USA, 2018. URL https://aip.scitation.org/doi/pdf/10.1063/1.5127684.

[13] K. Hock et al. *Imperfection resonance crossing in the AGS Booster*. C-AD Tech Note 633, 2020. URL https://www.osti.gov/servlets/purl/1661654.

[14] F. Meot et al. *On the image of AGS 3He2+ no in the blue*. AP Note 560, 2016. URL https://technotes.bnl.gov/PDF?publicationId=38802.

[15] V. Ptitsyn et al. EIC Hadron Spin Rotators. In *Proc. 13th International Partile Accelerator Conference (IPAC'22), Bangkok, Thailand*, 2022.

[16] V. Ptitsin et al. Helical spin rotators and snakes. *NIMA*, 1996.

[17] F. Meot et al. *Re-visiting RHIC snakes: OPERA fields, n0 dance*. AP Note 590, 2017. URL https://technotes.bnl.gov/PDF?publicationId=42159.